Progress In Electromagnetics Research, Vol. 141, 693–710, 2013

NOVEL MINIATURIZED KOCH PENTAGONAL FRACTAL ANTENNA FOR MULTIBAND WIRELESS APPLICATIONS

Omar M. Khan[1, *], Zain U. Islam[1], Imran Rashid[1], Farooq A. Bhatti[1], and Qamar U. Islam[2]

[1]Department of Electrical Engineering, College of Signals, National University of Sciences and Technology, Islamabad, Pakistan

[2]Department of Electrical Engineering, Institute of Space Technology, Islamabad, Pakistan

Abstract—A novel reduced size three band Koch Pentagonal fractal antenna is presented. The proposed antenna uses pentagonal shape for the basic fractalization combined with inner sides etched with Koch fractal pattern of the first iteration providing reduction in the overall size of the antenna. For higher order of iterations, more size reduction is achieved, producing equal number of radiation bands. Optimization is done for achieving radiations in the S, C and X bands. Ansoft HFSS, CST Microwave Studio and Solid Works are used for the 3D Modeling, S_{11} frequency optimization and radiation pattern calculations. The proposed third iteration fractal configuration is fabricated on Rogers RT5870, and measured results are presented. Size reduction up to 43.26 percent in terms of its overall size and 75.18 percent in terms of copper cladding remaining is achieved for the third iteration proposed fractal antenna in comparison to pentagonal patch antenna operating in the first resonant frequency band.

1. INTRODUCTION

The term fractal was originally conceived by Mandelbrot [1] to describe a family of complicated configurations that have repeatability in their shapes. The main motivation of fractal modeling comes from the many fractal shapes present in nature. For example, fractals have been magnificently used to model complex natural entities such as clouds, boundaries, coastlines, galaxies, mountain ranges, snowflakes, ferns,

Received 9 June 2013, Accepted 29 July 2013, Scheduled 9 August 2013

* Corresponding author: Omar Masood Khan (omar.khan@mcs.edu.pk).

trees, leaves and many more geometrical objects. There is an ever going demand in both military and commercial applications for antennas having the attributes of multiband behavior, compact size, conformal and low profile [2]. Fractal geometries with their complex iterative nature demonstrate these required attributes. The suitability of fractal antennas for multiband applications is thoroughly discussed in [3, 4]. An overview of different shapes including Koch snowflake/islands fractal iterations, Sierpinski gasket and carpets fractal stages, fractal trees and Hilbert curves is given in [2]. Pentagonal fractal shape has been proposed in [5]. Modified fractal geometries for improvement in antenna attributes have been reported in literature such as modified Koch Sierpinski fractal shapes and Koch like sided Sierpinski gasket antennas [6, 7]. Novel Giuseppe Peano fractal geometry is discussed in [8] for miniaturization purposes and its results are compared with Tee type, Sierpinski and Koch fractal geometries. In [9] the experimental and numerical analysis of Koch monopole is presented, where Q of antenna is compared with the number of iterations on Koch monopole. The relationship between current density distributions and modes are discussed in [10], with there application in directive patterns. Sierpinskized Koch-like sided bow-tie multifractal antenna is designed in [11], which is fed by microstrip Balun that is linearly tapered operating in six frequency bands. Sierpinski fractal structured carpet monopole antenna is designed using the technology of metallized foam in [12]. Several metallo-dielectric fractal based structures are studied for scattering behavior and for a range of frequencies the Sierpinski carpet based structure are found out to produce lower backscattering in [13]. CST is used to simulate the log periodic fractal Koch antenna at UHF in [14] with size reduction upto 27 percent is achieved by different number of iterations. In [15] Ku band broadband circularly polarized Spidron slotted fractal antenna array has been designed for satellite communication applications. Sierpinski-carpet fractals are chosen in [16] for bandwidth enhancement with the advantage of additional resonances. With the use of genetic algorithm, Sierpinski rectangular carpet antenna arrays are optimized for satellite communication links in [17]. The properties of bessel beams radiated by fractal conical lenses are analyzed using Stratton-Chu formulas and two-dimension finite difference time domain method in [18].

Modified Minkowski fractal configuration is applied to rhombic monopole patch antenna in [19] for radiations for wireless applications. Fractal shape is also used for reduction in mutual coupling between adjacent elements when placed in array configuration in [20]. Many different configurations of fractal shapes applied to antennas for size reduction and multiband behavior are described in [21–31].

This paper presents a novel Koch Pentagonal fractal antenna based on iteratively fractalizing pentagonal patch and simultaneously etching the inner sides of the pentagon with Koch fractal antenna of the 1st order for miniaturization and multiband behavior.

2. KOCH EMBEDDED PENTAGON CELL ANALYSIS

The novel approach of embedding first order Koch fractal geometry in the pentagonal patch antenna is used for achieving miniaturization in the overall size of the pentagon patch. With the increase in the size of first order Koch fractal, the metallic part of the antenna reduces, and the resonant frequency of the pentagon also tends to shift towards the lower frequencies. Simulations are done to analyze the exact effects of etching Koch fractal into the center of pentagon patch.

The single pentagon patch is designed according to the methodology available for microstrip antenna design from the following equations [6].

$$\epsilon_{reff} = \frac{\epsilon_r + 1}{2} + \frac{\epsilon_r - 1}{2}\left[1 + 12\frac{h}{\frac{v_o}{2f_r}\sqrt{\frac{2}{\epsilon_r+1}}}\right]^{-0.5} \tag{1}$$

$$L_{diff} = (0.412)h\frac{(\epsilon_{reff} + 0.3)\left(\frac{\frac{v_o}{2f_r}\sqrt{\frac{2}{\epsilon_r+1}}}{h} + 0.264\right)}{(\epsilon_{reff} - 0.3)\left(\frac{\frac{v_o}{2f_r}\sqrt{\frac{2}{\epsilon_r+1}}}{h} + 0.8\right)} \tag{2}$$

$$L_{pent} = \frac{v_o}{2f_r\sqrt{\epsilon_{reff}}} - 2L_{diff} \tag{3}$$

f_r is the first resonant frequency of 2.4 GHz, ϵ_r the dielectric constant of the substrate of value 2.33, h the height of the substrate taken as 1.575 mm, ϵ_{reff} the effective dielectric constant, L_{diff} the increase in length due to fringing effects, L_{pent} the length of each side of the pentagon calculated to be 40.22 mm, and v_o the free-space velocity of light. The HFSS labeled model of pentagon patch is shown in Figure 1(a), with the Koch embedded pentagon labeled HFSS model depicted in Figure 1(b). The Solid Works detailed dimensions drawing of the pentagon and Koch embedded pentagon are illustrated in Figures 1(c) and 1(d) respectively, where the pentagon patch lengths are optimized at 39.03 mm in CST, and their corresponding CST gain plot comparison is shown in Figure 1(e).

The effects of frequency responses of pentagon upon embedding the first Koch fractal geometry are analyzed in CST. The simulated

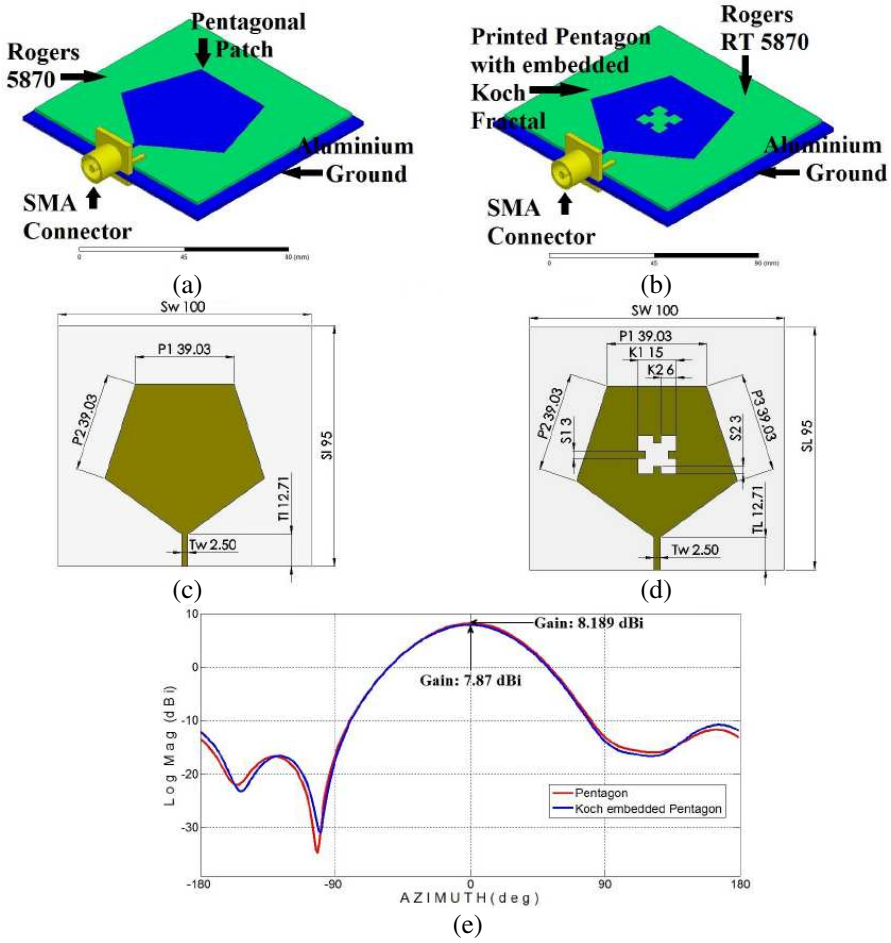

Figure 1. Pentagon patch and Koch embedded pentagonal patch antenna, HFSS labeled 3D models. (a) Pentagon patch antenna, (b) Koch pentagon patch antenna, Solid Works dimensions drawings, (c) pentagon patch antenna, (d) Koch pentagon patch antenna, (e) CST gain comparison of Pentagon and Koch embedded pentagon patch antennas.

frequency versus the S_{11} responses of pentagon antenna for different dimensions of embedded Koch fractal are shown in Figure 2. The variables sw and ow represent the Koch fractal length and slots respectively. It is evident from Figure 2 that as length of the Koch fractal is increased, the frequency response tends to shift towards lower

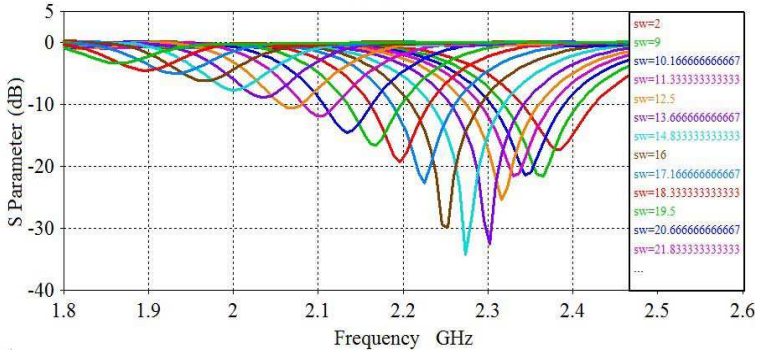

Figure 2. Frequency responses of pentagon antenna against different dimensions of embedded Koch fractal in CST.

frequency points. At Koch fractal length 2 mm, the frequency response is 2.37 GHz at −17.35 dB, whereas at Koch fractal length 30 mm, the frequency response is shifted down to 1.86 GHz at −3.42 dB. Hence there is a trade-off between the size reduction and antenna efficiency.

Effects of embedding different sizes of first order Koch fractal in the pentagon patch and its effects on the resonant frequency points of the pentagon patch are illustrated in Figure 3. The comparison of frequency responses for originally designed pentagon antenna at 2.4 GHz for WiFi applications and optimal Koch fractal pentagon antenna are shown in Figure 3(a). The relationship between the Koch fractal area, frequency and S_{11} response is depicted in Figure 3(b).

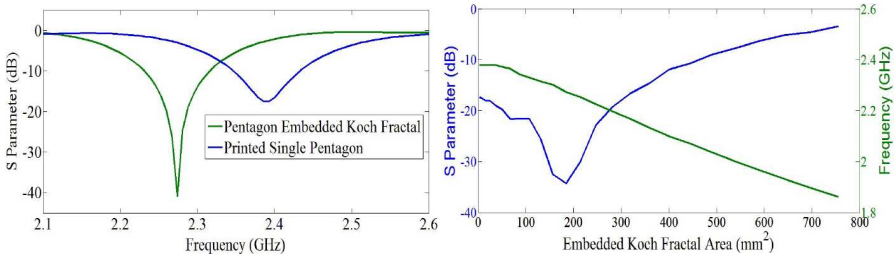

Figure 3. Koch fractal effects on the original antenna. (a) Frequency versus *s*-parameters of optimal selected Koch fractal embedded in pentagon against original pentagon, (b) fractal Koch area effects on *s*-parameters and frequency response of pentagon.

As depicted in Figure 3(b) the frequency tends to shift downwards starting from 2.37 GHz to 1.86 GHz as the Koch fractal area is increased from 3.36 mm sq. to 756 mm sq., respectively. It will require the size of the antenna to be reduced in order to tune the Koch pentagon antenna back to 2.4 GHz, thus its representing effects of Koch fractal area on size reduction of the pentagon antenna. Improved matching is an additional advantage of embedding the Koch fractal in the pentagon upto a certain increase in Koch fractal area and optimal value is selected for the further fractalization of the proposed third order geometry.

The empirical relation between the Koch embedded fractal area of the first order and the S parameters is determined by using Curve fitting tool of MATLAB. Equations (1), (2) and (3) gives the relation between Koch fractal area and S parameters with three different fit types of Gaussian, Fourier and Sum of Sine functions respectively. The corresponding calculated coefficients for the three fits are illustrated in Table 1. The Sum of squares due to error (SSE), Coefficient of determination (R-square), Degree-of-freedom adjusted coefficient of determination (Adjusted R-square) and Root mean squared error (RMSE) are found out to be 1.919, 0.9989, 0.9731, 1.385 for the Gaussian, 1.587, 0.9991, 0.9968, 0.4762 for the Fourier and 1.299, 0.9992, 0.9818, 1.14 for the Sum of Sine functions respectively.

$$\begin{aligned} f(x) = {} & a1\exp\left(-((x-b1)/c1)^2\right) + a2\exp\left(-((x-b2)/c2)^2\right) \\ & + a3\exp\left(-((x-b3)/c3)^2\right) + a4\exp\left(-((x-b4)/c4)^2\right) \\ & + a5\exp\left(-((x-b5)/c5)^2\right) + a6\exp\left(-((x-b6)/c6)^2\right) \\ & + a7\exp\left(-((x-b7)/c7)^2\right) + a8\exp\left(-((x-b8)/c8)^2\right) \end{aligned} \quad (4)$$

$$\begin{aligned} f(x) = {} & a0 + a1\cos(xw) + b1\sin(xw) + a2\cos(2xw) + b2\sin(2xw) \\ & + a3\cos(3xw) + b3\sin(3xw) + a4\cos(4xw) + b4\sin(4xw) \\ & + a5\cos(5xw) + b5\sin(5xw) + a6\cos(6xw) + b6\sin(6xw) \\ & + a7\cos(7xw) + b7\sin(7xw) + a8\cos(8xw) + b8\sin(8xw) \end{aligned} \quad (5)$$

$$\begin{aligned} f(x) = {} & a1\sin(b1x + c1) + a2\sin(b2x + c2) + a3\sin(b3x + c3) \\ & + a4\sin(b4x + c4) + a5\sin(b5x + c5) + a6\sin(b6x + c6) \\ & + a7\sin(b7x + c7) + a8\sin(b8x + c8) \end{aligned} \quad (6)$$

3. KOCH PENTAGONAL FRACTAL ANTENNA DESIGN

The proposed fractal geometry is designed for resonating at the first harmonic frequency of 2.4 GHz for the WIMAX and WIFI applications. The unit cell and first three iterations of the Koch fractal geometry and pentagonal fractal geometry is shown in Figures 4(a) and 4(b)

Table 1. Coefficients for different fit types.

Coefficients	Gaussian	Fourier	Sum of Sine Function
a0	–	$9.27E+04$	–
$a1$	-21.08	1971	26.26
$b1$	103.6	$-1.72E+05$	0.004372
$c1$	216.9	–	-3.233
$a2$	-5.414	$-1.36E+05$	2.762
$b2$	155.4	-3037	0.01858
$c2$	26.15	–	1.771
$a3$	-11.6	-2893	16.46
$b3$	192.8	$9.07E+04$	0.007834
$c3$	41.52	–	-2.131
$a4$	-3.44	$5.04E+04$	16.06
$b4$	263.1	2006	0.03968
$c4$	84.52	–	-4.591
$a5$	2.932	1042	58.3
$b5$	472.1	$-2.26E+04$	0.04374
$c5$	113.4	–	-2.999
$a6$	-11.47	-7751	112
$b6$	451.8	-402.3	0.04949
$c6$	195.2	–	7.584
$a7$	0	-113.5	129.4
$b7$	616.4	1830	0.04743
$c7$	3.713	–	5.14
$a8$	-2.643	225.1	25.45
$b8$	729.9	19.89	0.05266
$c8$	86.47	–	3.381
w	–	0.004405	–

respectively. The proposed Koch pentagonal fractal configuration is demonstrated in Figure 4(c). Unit cell of this fractal consists of the pentagonal patch which is etched from the inside based on optimally selected first order Koch fractal geometry.

The 1st iteration of the Koch pentagonal fractal antenna is shown in Figure 4(c). For achieving the first fractal iteration the basic Koch pentagon is transformed into five smaller scaled Koch pentagons. The total number of 1st order Koch fractals used in the 1st iteration of Koch

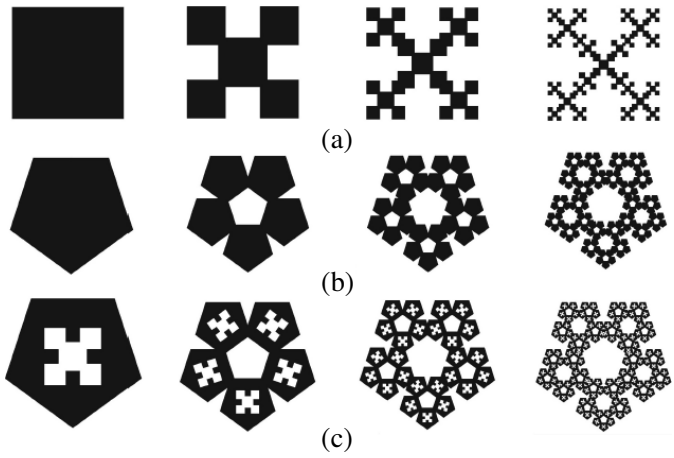

Figure 4. Cell and first three iterations of (a) Koch fractal geometry, (b) pentagonal fractal geometry, (c) proposed Koch embedded pentagonal fractal geometry.

pentagonal fractal are five as shown in Figure 4(c). The pentagons are scaled at the ratio of 2/5 corresponding to scaling factor of 0.4. The inner Koch fractal of the 1st iteration is scaled in comparison to the Koch fractal for the basic cell at ratio of 2/5.

The 2nd iteration for the Koch pentagonal fractal geometry is depicted in Figure 4(c). The five Koch pentagons of the 1st iteration are fractalized into 25 Koch pentagons. Each Koch pentagon of the 1st iteration is fractalized into five Koch pentagons at the ratio of 2/5. The overall scaling of the 25 Koch pentagons of the 2nd iteration is at the ratio of 4/25 in comparison with the Koch pentagon of the basic cell. The Koch fractal of the 1st iteration etched in the center of the pentagon is scaled at the ratio of 4/25 with respect to the Koch fractal of the 1st iteration used in the basic cell. This inner Koch fractal of the 1st order for the 2nd iteration of Koch pentagonal fractal geometry is at the ratio of 2/5 with respect to inner 1st order Koch fractal used in the 1st iteration of Koch pentagonal fractal, hence giving a symmetry in the ratios with which both the main pentagon and inner 1st order Koch are fractalized from 1st iteration of the Koch fractal geometry to 2nd iteration. The total number of inner 1st order Koch fractals used in the 2nd order of Koch pentagonal fractal geometry are 25 as depicted in Figure 4(c). The 3rd iteration of the Koch pentagonal fractal antenna is shown in Figure 4(c). The 25 Koch pentagons of the 2nd order Koch pentagonal fractal geometry are fractalized into 125 scaled down Koch pentagons as depicted in Figure 4(c). The overall scaling of these 125 Koch pentagons used in the 3rd iteration of Koch pentagonal fractal

geometry is at the ratio of 8/125, 4/25 and 2/5 in comparison with the Koch pentagon of the basic cell, Koch pentagonal fractal geometry of the 1st iteration and Koch pentagonal fractal geometry of the 2nd iteration respectively. The Koch fractals of the 1st iteration etched into the center of the Koch pentagons used in the 3rd iteration of the Koch pentagonal fractal geometry as shown in Figure 4(c), are at the ratio of 8/125, 4/25 and 2/5 in comparison with the Koch fractal of 1st iteration used in the center of the basic cell of Koch pentagon fractal geometry, 1st iteration of the Koch pentagonal fractal geometry and 2nd iteration of the Koch pentagonal fractal geometry respectively. The total number of 1st order Koch fractals used in the 3rd iteration of the Koch pentagonal fractal geometry is 125.

4. SIMULATION AND MEASURED RESULTS

The proposed fractal antenna is designed to achieve desired resonant points in S, C and X frequency bands. In these frequency bands, the Koch pentagonal fractal antenna can be tuned to a wide range of frequency points according to specific applications. For demonstrating the frequency tuning capability of the proposed antenna six different scaled third iteration fractal configurations are illustrated in Figure 5. The variables cr, $cr2$ and $cr3$ represent the radii of cell, first order and

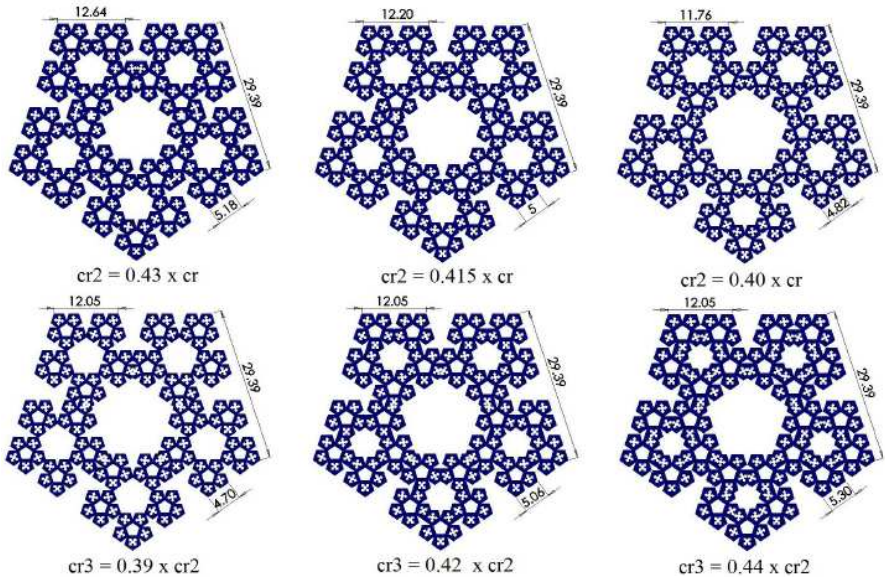

Figure 5. Third iteration proposed fractal antenna geometries with different scaling factors for $cr2$ and $cr3$ for controlling frequency bands.

second order of Koch pentagon fractals respectively. The tuning of frequency points in the C and X bands are illustrated in Figures 6(a) and 6(b) respectively with the range of tuning in these bands are shown upto 600 MHz and 1 GHz respectively. The desired frequency points in these bands are precisely controlled by selecting the optimal scaling factors for cr, $cr2$ and $cr3$ in the proposed Koch pentagon fractal antenna.

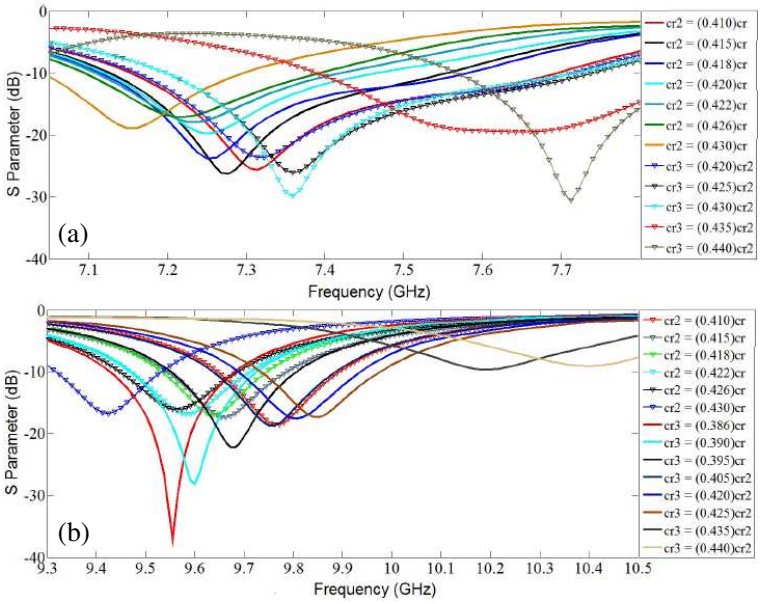

Figure 6. Demonstration of frequency tuning capability of proposed fractal geometry at different frequencies in (a) C band, (b) X band.

The proposed antenna third iteration fractal antenna 3D HFSS labeled model, Solid Works dimensions drawing, and fabricated prototype are shown in Figures 7(a), 7(b) and 7(c), respectively. The proposed antenna is designed on Rogers RT5870 with dielectric constant 2.33, thickness 1.575 mm, and loss tangent 0.0012. The height of the ground plane is optimized for achieving maximum bandwidth and gain efficiency. The dimension details along with their descriptions are listed in Table 2. The area of the proposed fractal antenna is 1487.54 mm in terms of its overall size and 650.79 mm sq in terms of copper remaining and the area of original pentagon patch antenna is calculated to be 2622.07 mm sq.

Hence there is a size reduction of 43.26 percent in terms of its overall size and 75.18 percent in terms of copper remaining. The

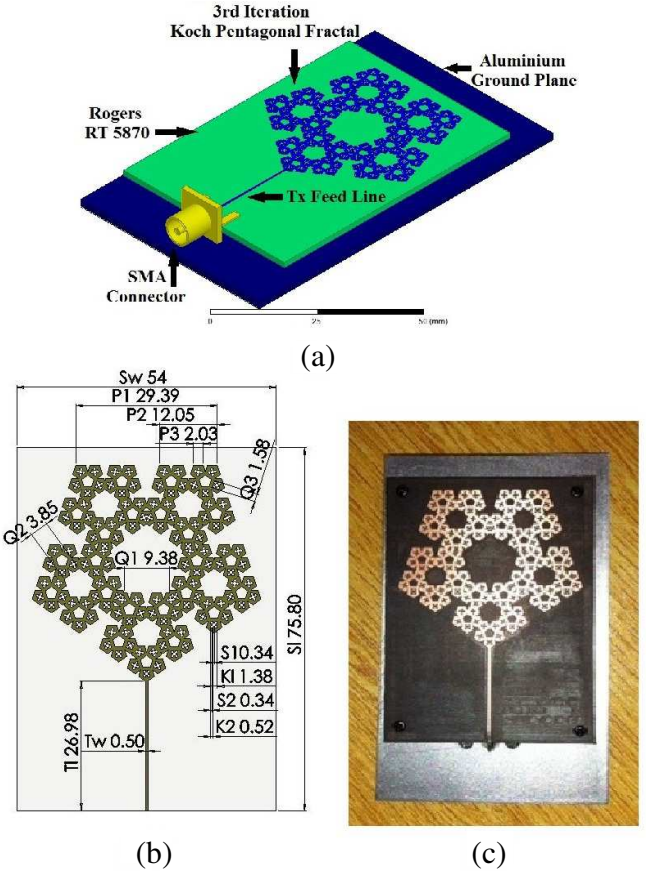

Figure 7. Proposed third iteration Koch embedded pentagonal fractal antenna. (a) HFSS 3D labeled model, (b) Solid Works dimensions drawing, (c) fabricated prototype.

third iteration fractal antenna is designed to operate for S, C and X Band applications. Measured and CST simulated S_{11} responses of the proposed fractal antenna with the desired frequency bands achieved by optimizing the ratios of $cr2$ and $cr3$ are shown in Figure 8(a). CST simulated real, imaginary, magnitude and phase plots for the input impedance versus the three frequency bands of the proposed fractal geometry are shown in Figure 8(b).

Third iteration Koch pentagonal fractal antenna E-field, H-field, surface current and current density plots are illustrated in Figure 9 for S, C and X band frequencies. The z component of the E-

Table 2. Third iteration Koch pentagonal fractal antenna descriptions.

Label	Description	Dimension mm
S_w	Substrate Width	54
S_l	Substrate Length	75.8
P_1	1st Pentagon Length	29.39
P_2	2nd Pentagon Length	12.05
P_3	Third Pentagon Length	2.03
Q_1	Inner 1st Polygon Length	9.38
Q_2	Inner 2nd Polygon Length	3.85
Q_3	Inner 3rd Pentagon Length	1.58
S_1	Koch Fractal Slot Length	0.34
S_2	Koch Fractal Slot Width	0.34
K_1	Koch Fractal overall Length	1.38
K_2	Koch Fractal Inner Square Length	0.52
T_w	Transmission Line Width	0.5
T_l	Transmission Line Length	26.98

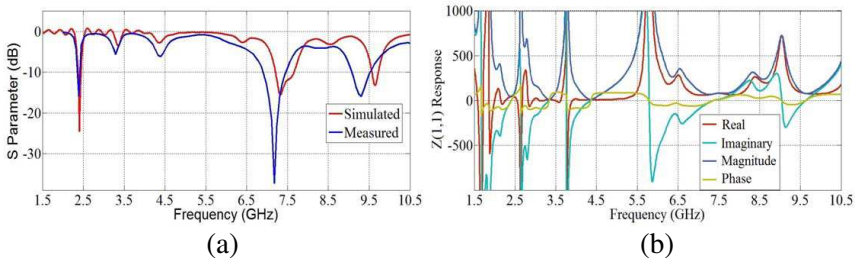

Figure 8. Plots for third iteration Koch pentagon fractal antenna. (a) CST simulated and measured S_{11} parameter responses, (b) CST input impedance responses.

field for 2.4 GHz is shown in Figures 9(a) and 9(b) for current flow along x-axis with phases 0 and 180 degrees, respectively. At 2.4 GHz the fractal antenna is radiating as a whole which is representing the first resonance of the fractal antenna. For radiations of the proposed fractal antenna in the second band of radiation the second order Koch fractals are radiating as a single unit as seen by the radiation of the antenna in the z component of E-field at 7.4 GHz in

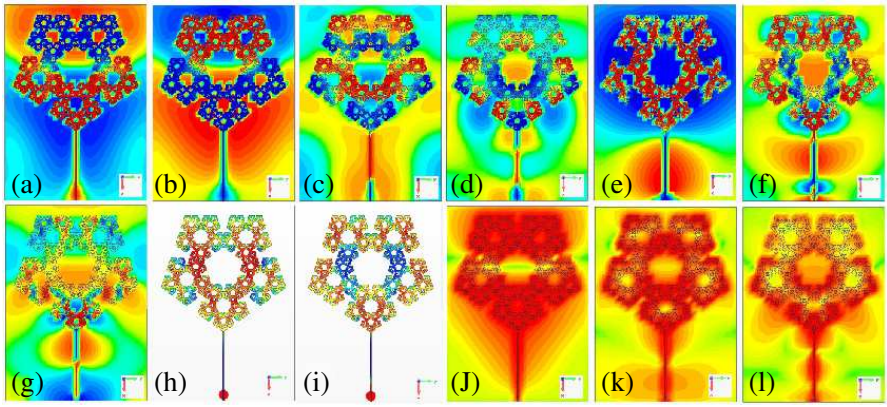

Figure 9. Third iteration Koch pentagonal fractal antenna, E-fields at frequencies (a) 2.4 GHz at phase 0 deg, (b) 2.4 GHz at phase 180 deg, (c) 7.4 GHz, (d) 9.2 GHz; H-fields at frequencies (e) 2.4 GHz, (f) 7.4 GHz, (g) 9.2 GHz; Surface currents at frequencies (h) 2.4 GHz, (i) 7.4 GHz and current densities at frequencies (j) 2.4 GHz, (k) 7.4 GHz, (l) 9.2 GHz.

Figure 9(c) and for the radiations in third band, the third order Koch pentagon units are radiating as demonstrated in Figure 9(d) from the z component of E-field at 9.2 GHz. The y components of the H-fields of Figures 9(e), 9(f) and 9(g) are showing the radiations of the proposed fractal antenna as a result of the radiation of the complete fractal unit, the second order Koch pentagon units and third order Koch pentagon units respectively thus producing resonances in S, C and X bands respectively. The surface currents at frequencies 2.4 GHz and 7.4 GHz are shown in Figures 9(h) and 9(i) respectively. The current densities at frequencies 2.4 GHz, 7.4 GHz and 9.2 GHz are shown in Figures 9(j), 9(k) and 9(l) respectively. For the first resonance at 2.4 GHz the current is concentrated in the Koch pentagons as a whole with no current flow at the center of the fractal antenna thus producing the first resonance of the proposed antenna. The current density at 7.4 GHz in Figure 9(k) is concentrated along the inner and outer regions of the Koch fractal pentagons of the second iteration which represents the radiation of the antenna in the second frequency band, with little current flowing at the inner areas of the whole Koch pentagon. For the frequency of 9.2 GHz, the current density concentration in Figure 9(l) is along the smallest length Koch pentagons designed for the third iteration of the Koch pentagonal fractal geometry, having no currents concentrated along the inner or outer sides of the Koch pentagon

fractals designed for the second iteration of the fractal configuration thus representing the resonance of the antenna in the third frequency band.

The three-dimensional CST gain plots for the third iteration Koch pentagonal fractal antenna are shown in Figure 10 for S, C and X frequency bands. Comparison of measured vs simulated gain plots in the S, C and X bands are illustrated in Figure 11 and detailed measured gain patterns and gain vs frequency for the S, C and X bands are shown in Figure 12.

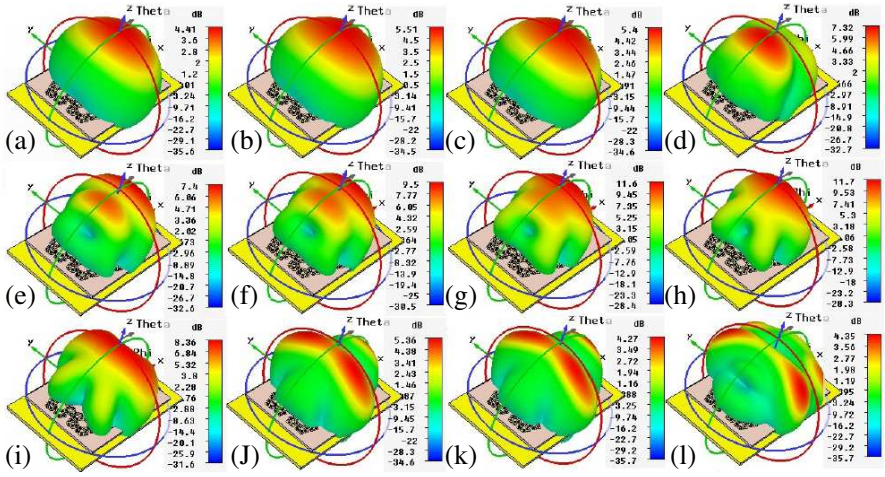

Figure 10. Third iteration Koch pentagonal fractal antenna 3D CST gain plots at frequencies (a) 2.32 GHz, (b) 2.385 GHz, (c) 2.42 GHz, (d) 6.4 GHz, (e) 6.84 GHz, (f) 7.0 GHz, (g) 7.2 GHz, (h) 7.5 GHz, (i) 7.8 GHz, (j) 8.75 GHz, (k) 8.82 GHz, (l) 9.3 GHz.

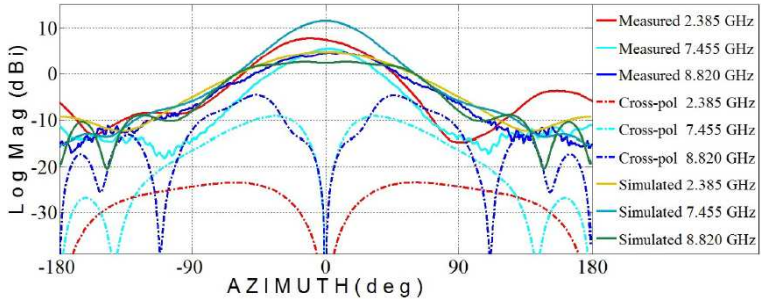

Figure 11. Measured vs simulation gain plots in S, C and X frequency bands of third order Koch pentagonal fractal antenna.

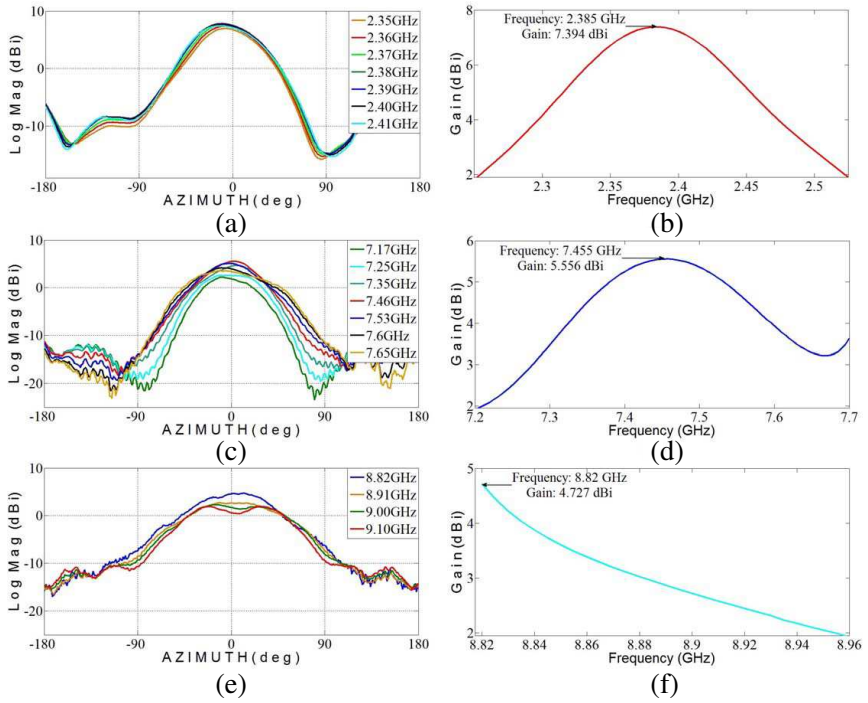

Figure 12. Detailed measured gain plots for the third iteration Koch pentagonal fractal antenna in different frequency bands; S band (a) gain plots at different frequencies, (b) gain vs frequency plot, C band (c) gain plots at different frequencies, (d) gain vs frequency plot, X band (e) gain plots at different frequencies, (f) gain vs frequency plot.

5. CONCLUSION

The multiband novel Koch pentagonal fractal antenna has been presented for wireless communication applications. The proposed novel third iteration Koch fractal antenna is designed, modeled, simulated, fabricated, tested and verified for the radiation characteristics in S, C and X Bands. Novel methodology for controlling the desired frequency points from the proposed Koch pentagonal fractal antenna is presented. The antenna exhibits good matching and radiation efficiencies across the bands specified. The concept of size reduction with the use of fractal geometry has been validated in comparison with conventional pentagonal patch antenna.

REFERENCES

1. Mandelbrot, B. B., *Fractals: Form, Chance and Dimension*, W. H. Freeman, 1977, ISBN 0-7167-0473-0.
2. Werner, D. H. and S. Ganguly, "An overview of fractal antenna engineering research," *IEEE Antennas and Propagation Magazine*, Vol. 45, No. 1, 38–57, Feb. 2003.
3. Puente, C., J. Romeu, R. Pous, X. Garcia, and F. Benitez, "Fractal multiband antenna based on Sierpinski gasket," *Electron. Lett.*, Vol. 32, No. 1, 1–2, Jan. 1996.
4. Puente-Baliarda, C., J. Romeu, R. Pous, and A. Cardama, "On the behavior of the Sierpinski multiband fractal antenna," *IEEE Transactions on Antennas and Propagation*, Vol. 46, No. 4, 517–524, Apr. 1998.
5. Tang, P. W. and P. F. Wahid, "Fractal multiband antennas based on polygons," *Antennas and Propagation Society International Symposium*, Vol. 4, 230–233, 2003.
6. Yu, Z.-W., G.-M. Wang, X.-J. Gao, and K. Lu, "A novel small-size single patch microstrip antenna based on Koch and Sierpinski fractal-shapes," *Progress In Electromagnetics Research Letters*, Vol. 17, 95–103, 2010.
7. Li, D. and J.-F. Mao, "Koch-like sided Sierpinski gasket multifractal dipole antenna," *Progress In Electromagnetics Research*, Vol. 126, 399–427, 2012.
8. Oraizi, H. and S. Hedayati, "Miniaturization of microstrip antennas by the novel application of the Giuseppe Peano fractal geometries," *IEEE Transactions on Antennas and Propagation*, Vol. 60, No. 8, 3559–3567, Aug. 2012.
9. Baliarda, C. P., J. Romeu, and A. Cardama, "The Koch monopole: A small fractal antenna," *IEEE Transactions on Antennas and Propagation*, Vol. 48, No. 11, 1773–1781, Nov. 2000.
10. Borja, C. and J. Romeu, "On the behavior of Koch island fractal boundary microstrip patch antenna," *IEEE Transactions on Antennas and Propagation*, Vol. 51, No. 6, 1281–1291, Jun. 2003.
11. Li, D. and J.-F. Mao, "Sierpinskized Koch-like sided multifractal dipole antenna," *Progress In Electromagnetics Research*, Vol. 130, 207–224, 2012.
12. Anguera, J., J. P. Danial, C. Borja, J. Mumbru, C. Puente, T. Leduc, K. Sayegrith, and P. Van Roy, "Metallized foams for antenna design: Application to fractal-shaped Sierpinski-carpet monopole," *Progress In Electromagnetics Research*, Vol. 104, 239–251, 2010.

13. Chandran, A. R., M. Gopikrishna, C. K. Aanandan, P. Mohanan, and K. Vasudevan, "Scattering behaviour of fractal based metallo-dielectric structures," *Progress In Electromagnetics Research*, Vol. 69, 323–339, 2007.
14. Karim, M. N. A., M. K. Abd Rahim, H. A. Majid, O. B. Ayop, M. Abu, and F. Zubir, "Log periodic fractal Koch antenna for UHF band applications," *Progress In Electromagnetics Research*, Vol. 100, 201–218, 2010.
15. Trinh-Van, S., H. B. Kim, G. Kwon, and K. C. Hwang, "Circularly polarized Spidron fractal slot antenna arrays for broadband satellite communications in ku-band," *Progress In Electromagnetics Research*, Vol. 137, 203–218, 2013.
16. De la Mata Luque, T. M., N. R. Devarapalli, and C. G. Christodoulou, "Investigation of bandwidth enhancement in volumetric left-handed metamaterials using fractals," *Progress In Electromagnetics Research*, Vol. 131, 185–194, 2012.
17. Siakavara, K., "Novel fractal antenna arrays for satellite networks: Circular ring Sierpinski carpet arrays optimized by genetic algorithms," *Progress In Electromagnetics Research*, Vol. 103, 115–138, 2010.
18. Yu, Y.-Z. and W.-B. Dou, "Properties of approximate bessel beams at millimeter wavelengths generated by fractal conical lens," *Progress In Electromagnetics Research*, Vol. 87, 105–115, 2008.
19. Mahatthanajatuphat, C., S. Saleekaw, and P. Akkaraekthalin, "A rhombic patch monopole antenna with modified Minkowski fractal geometry for UMTS, WLAN and mobile WIMAX application," *Progress In Electromagnetics Research*, Vol. 89, 57–74, 2009.
20. Yousefzadeh, N., C. Ghobadi, and M. Kamyab, "Consideration of mutual coupling in a microstrip patch array using fractal elements," *Progress In Electromagnetics Research*, Vol. 66, 41–49, 2006.
21. Romeu, J. and J. Solar, "Generalized Sierpinski fractal multiband antenna," *IEEE Transactions on Antennas and Propagation*, Vol. 49, No. 8, 1237–1239, Aug. 2001.
22. Kim, I.-K., J.-G. Yook, and H.-K. Park, "Fractal-shape small size microstrip antenna," *Microwave and Optical Technology Letters*, Vol. 34, No. 1, 15–17, Jul. 5, 2002.
23. Anguera, J., C. Puente, C. Borja, R. Montero, and J. Soler, "Small and high-directivity Bow-Tie patch antenna based on the Sierpinski fractal," *Microwave and Optical Technology Letters*, Vol. 31, No. 3, 239–241, Nov. 5, 2001.

24. Chen, W.-L., G.-M. Wang, and C.-X. Zhang, "Small-size microstrip patch antennas combining Koch and Sierpinski fractal-shapes," *IEEE Antennas and Wireless Propagation Letters*, Vol. 7, 738–741, 2008.
25. Kim, J.-H., I.-K. Kim, J.-G. Yook, and H.-K. Park, "A slow-wave structure with Koch fractal slot loops," *Microwave and Optical Technology Letters*, Vol. 34, No. 2, 87–88, Jul. 20, 2002.
26. Puente, C., J. Romeu, R. Pous, J. Ramis, and A. Hijazo, "Small but long Koch fractal monopole," *Electron. Lett.*, Vol. 34, No. 1, 9–10, Jan. 1998.
27. Mirzapour, B. and H. R. Hassani, "Size reduction and bandwidth enhancement of snowflake fractal antenna," *IET Microwave Antennas Propagation*, Vol. 2, No. 2, 180–187, 2008.
28. Sinha, S. N. and M. Jain, "A Self-affine fractal multiband antenna," *IEEE Antennas and Wireless Propagation Letters*, Vol. 6, 110–112, 2007.
29. Hwang, K. C., "A modified Sierpinski fractal antenna for multi-band application," *IEEE Antennas and Wireless Propagation Letters*, Vol. 6, 357–360, 2007.
30. Li, D. and J. F. Mao, "A Koch-like sided fractal bow-tie dipole antenna," *IEEE Transactions on Antennas and Propagation*, Vol. 60, No. 5, 2242–2251, May 2012.
31. Song, C. T. P., P. S. Hall, and H. Ghafouri-Shiraz, "Perturbed Sierpinski multiband fractal antenna with improved feeding technique," *IEEE Transactions on Antennas and Propagation*, Vol. 51, No. 5, 1011–1017, May 2003.